Changes in very extreme precipitation due to global warming in a large ensemble by 60-km AGCM

Ryo Mizuta (Meteorological Research Institute, Japan, rmizuta@mri-jma.go.jp)

d4PDF: database for Policy Decision making for Future climate change

1. Introduction

- **Needs for high-resolution climate models**
  - High-resolution climate models can simulate frequencies of **regional-scale extreme events**, such as heavy rainfall and tropical cyclones, and their **changes due to global warming**.
  - We have been using a high-resolution AGCM, in which SST changes from CMIP climate models are prescribed. They are already used for impact assessment studies, with further dynamical downscaling to a regional climate model.

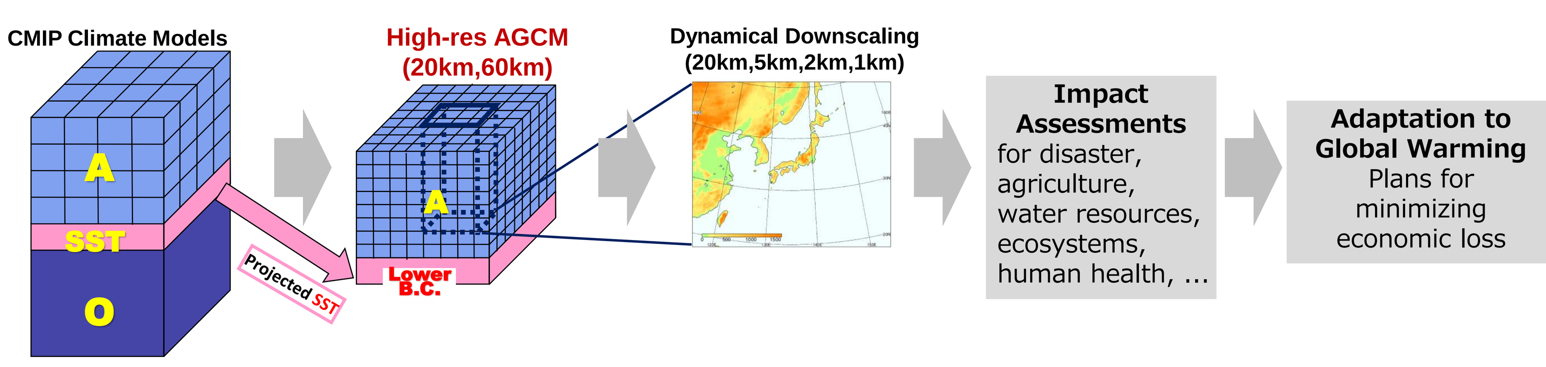

- **Requirements for high-resolution large ensemble simulations**
  - However, **uncertainties** of the change are larger for smaller-scale events and low-frequency events, although such events can have the most significant impacts on human activity.
  - In this study, **large-size** and **long-term** ensemble simulations with **high-resolution** models enables us to evaluate long-term changes in localized rare events that cannot be represented by coarse-resolution models and small-size ensembles.

	Multi-model ensemble	Single-model large ensemble
Global, large scale	CMIP experiments using ESMs	ESM Large ensemble
Regional scale	HighResMIP experiments	**High-resolution Large Ensemble = this study**

2. Simulation Data: d4PDF

- **d4PDF** http://www.miroc-gcm.jp/~pub/d4PDF/
  - MRI-AGCM3.2 with 60km resolution
- **Historical Simulations**
  - 60 years (1951–2010), 100 members
  - Observational sea-surface temperature (SST), sea-ice concentration, greenhouse gases, .. are prescribed as the boundary conditions.
- **+4K Simulations**
  - Climate when global-mean surface temperature is 4K warmer than pre-Industrial
  - 60 years, 90 members (6×15)
  - Future SST = detrended past SST + 6 SST warming patterns (ΔSST) from 6 CMIP5 models in RCP8.5 scenario
  - Each ΔSST has 15 ensemble members
  - Greenhouse gases are values in 2090 following RCP8.5 scenario

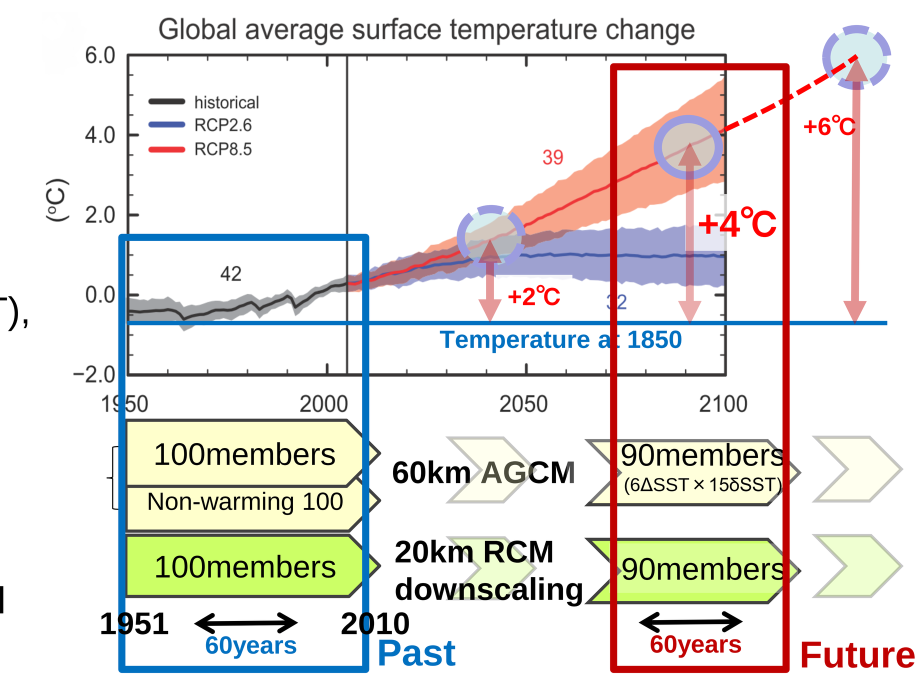

- **Thermodynamic and dynamic contributions to the increase in precipitation extremes**
  - Atmospheric variables (temperature, specific humidity, etc.) are composited over the days with extreme precipitation at each gridpoint.
  - Extreme precipitation estimated from these variables (O'Gorman and Schneider 2009; Pfahl et al. 2017):

$$P_e \sim -\left\{ \omega_e \frac{dq_s}{dp}\Big|_{\theta^*} \right\}$$

shows good approximation (a,b).
(ω_e: vertical wind; q_s: saturation specific humidity; θ^*: saturation equivalent potential temperature; { }: vertical integration)
  - The thermodynamic contribution (c) increases throughout the globe, whereas the dynamical contribution (d) determines the approximate geographic distribution.
  - Both contributions are approximated by the changes in the surface specific humidity and vertical wind at 500 hPa (e,f).

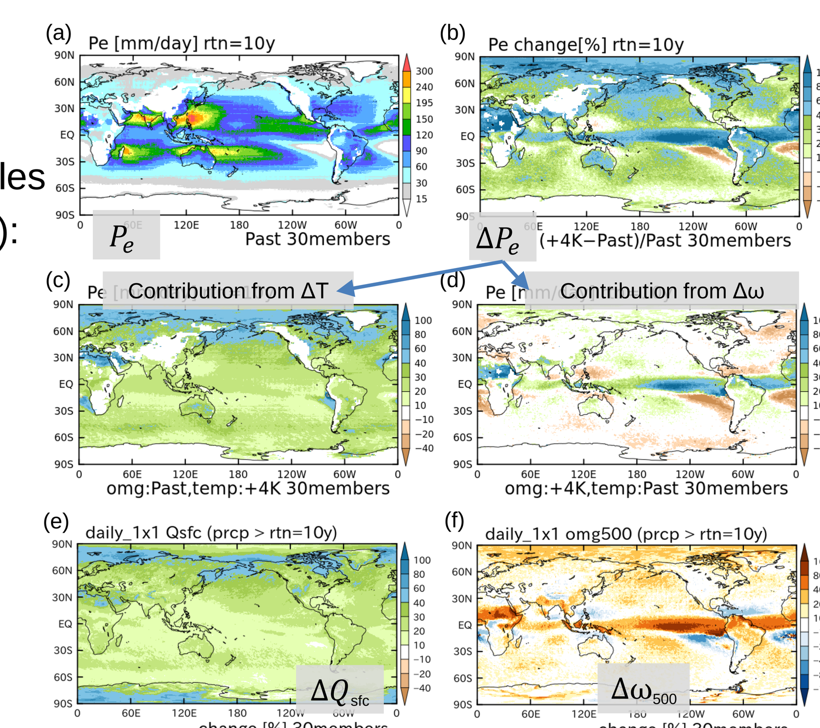

Fig.4: (a) 10-year return value of max. daily precipitation estimated from composited atmospheric variables (P_e), (b) changes in Pe in +4K experiments, (c) P_e changes due to temperature change, (d) P_e changes due to vertical wind change, (e) changes in surface specific humidity, and (f) changes in vertical wind at 500hPa.

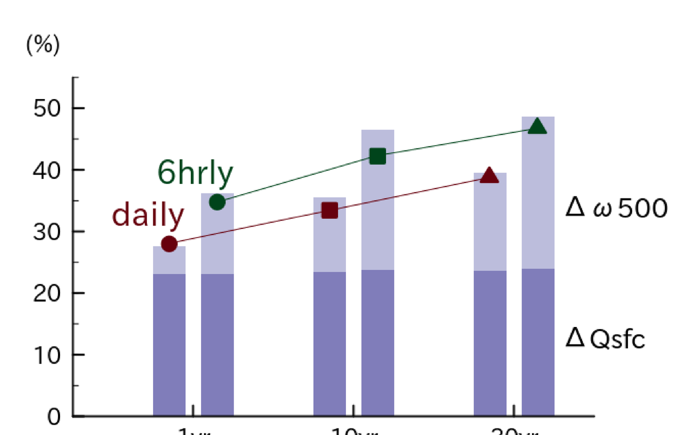

Fig.5: (bars) global average of the rate of increase in surface specific humidity and vertical wind at 500 hPa, with (lines) global-mean extreme precipitation increase, same as Fig.3.

- Surface specific humidity change is almost constant in any case, following C-C relationship.
- Vertical wind change is clearly larger in the case of shorter time scale and longer return period.
- The sum of the two is close to the extreme precipitation increase rate.

- On the events of longer return period, upward motion is more enhanced in upper troposphere (200-600hPa), accompanied by increase in horizontal convergence in mid troposphere (400-850hPa).

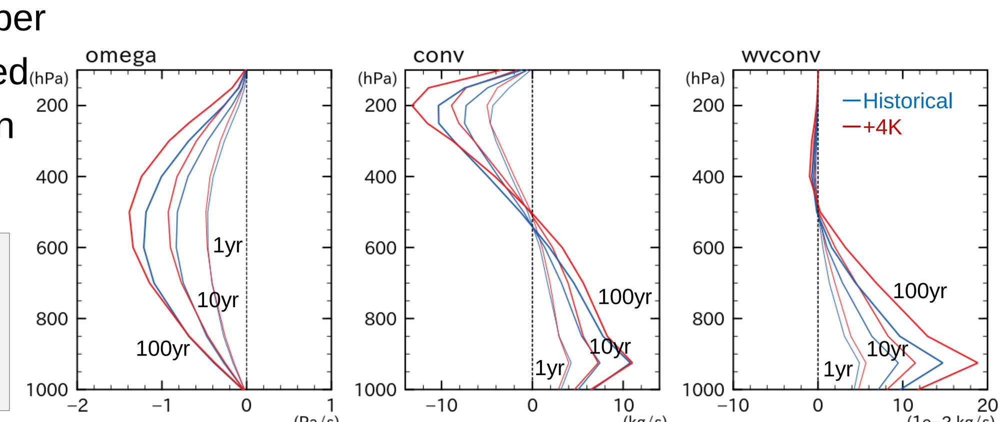

Fig.6: Vertical profiles of global-mean vertical wind, horizontal convergence, and horizontal water vapor convergence, composited over the days with extreme precipitation

3. Precipitation Extremes

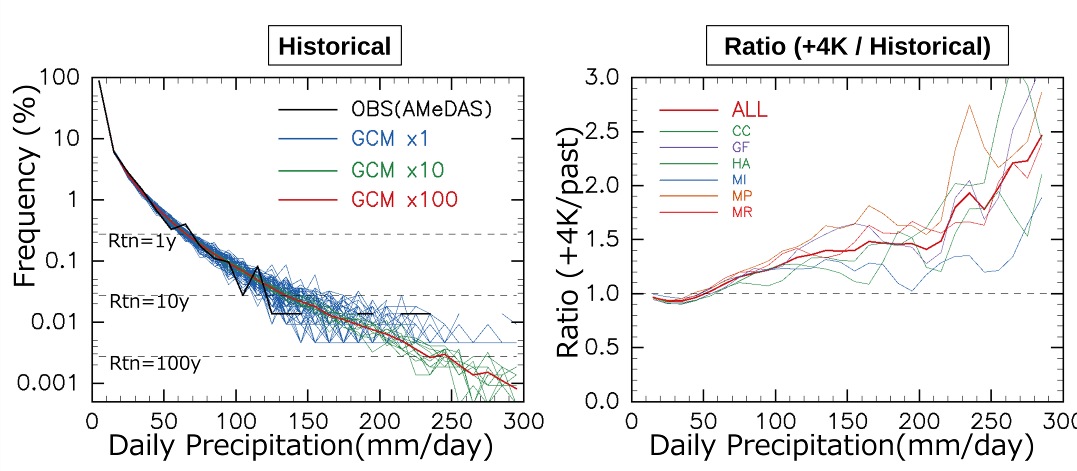

Fig.1: Frequency distribution of daily precipitation at Tokyo, (left) for the historical simulation and (right) change ratio from the historical to the +4K experiments.

- **Frequency distribution of daily precipitation at Tokyo**
  - Ensemble spread between members (Blue) is large in rare events.
  - Observation (Black) is inside the ensemble spread without any bias corrections.
  - Results from the total 100 members (Red) shows reasonable frequencies of extremes as low as 0.003%(=once in 100 years).
  - Increase is larger in the heavier precipitation rate.

- **1,10,100-year return value of daily precipitation**
  - Clear and smooth picture can be obtained by using large ensembles.
  - Future increase is found over most of the world about 20-40 % for the 10-year return value, and more for the 100-year return value.

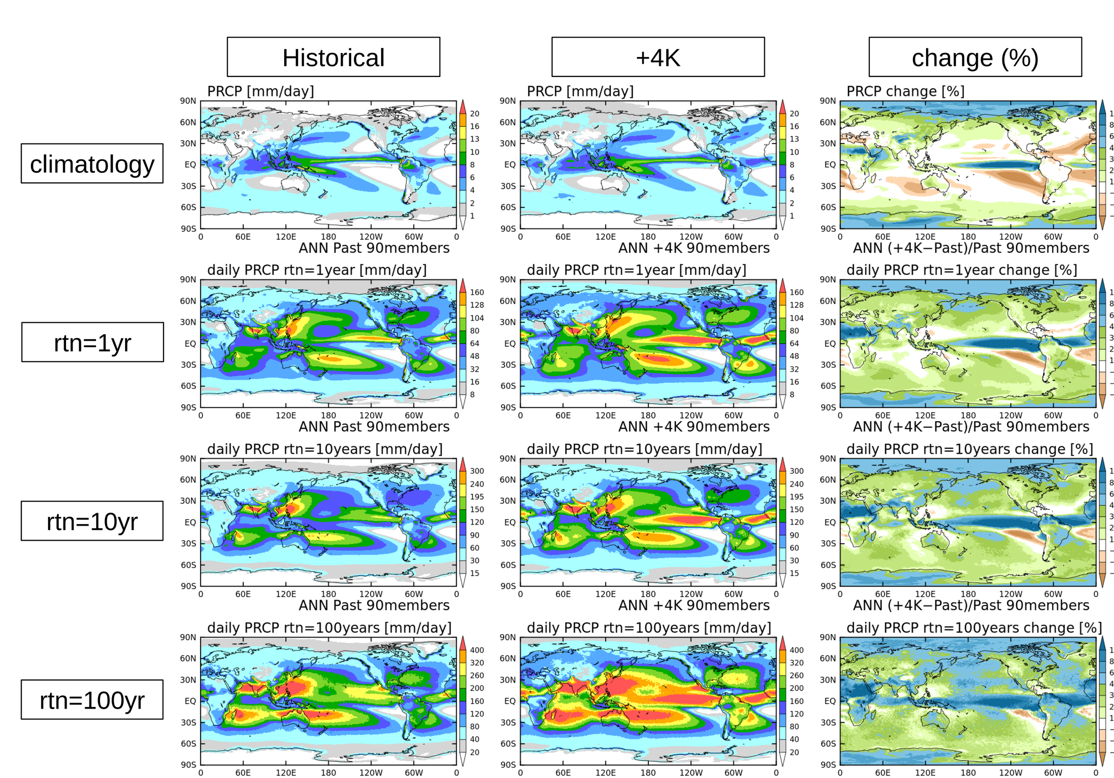

Fig.2: 1,10,100-year return value of daily precipitation (mm/day) and its change in the +4K simulation.

- **Dependence on return periods, time/spatial scales**
  - Larger increase in longer return period (i.e. rare events with heavy precipitation)
  - Larger increase in shorter time scale
  - Not so large dependence on spatial scale of the events
  - In any cases, the increase is larger than expected from Clausius-Clapeyron relationship (7%/K×3.6K =25%)

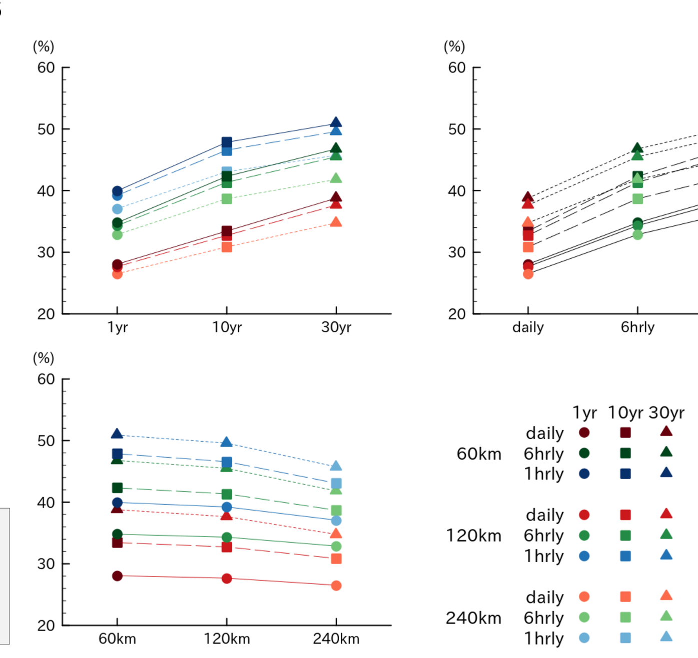

Fig.3: Global average of the rate of increase in extreme precipitation, for different return values, different time scales, and different spatial scales.

Acknowledgments
The calculations were performed on the Earth Simulator of the Japan Agency for Marine-Earth Science and Technology (JAMSTEC). This work was conducted under the TOUGOU Program of the Ministry of Education, Culture, Sports, Science and Technology (MEXT) of Japan.

5. Summary

- **Projected changes in very extreme precipitation events are investigated using d4PDF**
  - The rate of increase in precipitation is larger for less frequent (i.e. longer return period, heavier precipitation) events, and larger for shorter time-scale events.
  - Global average and geographical pattern of the increase cannot be explained by the increase of saturated water vapor content (~7%/K) following the Clausius-Clapeyron (C-C).
- **Temperature and vertical wind composited over the days of the events on every grid point**
  - Contributions by thermodynamics and dynamics are estimated.
  - While the thermodynamic contribution always obeys the C-C relationship in any return periods, the dynamic contribution, due to the vertical wind change, determines the geographical pattern, and the difference of increases between different return periods and different time scales.